New Fluorenyl-Substituted Dioxotetraamine Ligands and Their Copper(II) Complexes − Crystal Structure and Fluorescent Sensing Properties in Aqueous Solution

Li-Jian Jiang,[a,b] Qin-Hui Luo,*[a] Qing-Xiang Li,[a] Meng-Chang Shen,[a] and Hong-Wen Hu[a]

Keywords: Copper / Dioxotetraamines / Fluorescence / N ligands

Two new ligands consisting of a fluorenyl and dioxotetraaza unit, namely, 2,10-diamino-6-(9*H*-fluoren-9-yl)-4,8-diazaundecane-5,7-dione (L^1) and 1-(9*H*-fluoren-9-yl)-1,4,7,10-tetraazadecane-5,6-dione (L^2) along with their copper(II) complexes have been synthesized. Their properties were examined by ES-MS and CV in aqueous solution and the crystal structure of the copper(II) complex of L^1 has also been determined. The recognition of the transition metal ions (Cu^{2+}, Ni^{2+}, etc.) by receptors has been studied in aqueous solutions using pH-potentiometric and fluorimetric titrations. The results show that the binding of Cu^{2+} or Ni^{2+} ion with L^1 leads to quenching of the fluorescence of the fluorenyl group, but on the contrary the fluorescence of L^2 is enhanced. The mechanisms are discussed.

Introduction

The phenomena of luminescence quenching and enhancement resulting from metal−ligand interactions have attracted much attention with regards to its application in sensing metal ions in solution.[1,2] The dioxotetraamine ligands are interesting because they coordinate metal ions with the release of two protons on the amide nitrogen atoms and are able to stabilize a +3 oxidation state of transition metal ions.[3] Recently, chemists have been devoted to append a luminophore to the framework of the dioxotetraamine ligands and to explore new fluorescent signaling systems.[4−6] Although many luminescent signaling systems have been presented,[7−9] to date, hydrophilic luminescent ligands used as receptors are still rarely reported.[1,10] In view of the high quantum yield and long fluorescent lifetime of fluorene, we linked it as a luminophore to the dioxotetraamine units and obtained two new water-soluble ligands, 2,10-diamino-6-(9*H*-fluoren-9-yl)-4,8-diazaundecane-5,7-dione (L^1) and 1-(9*H*-fluoren-9-yl)-1,4,7,10-tetraazadecane-5,6-dione (L^2) and synthesized their complexes $[Cu(H_{-2}L^1)]\cdot 2H_2O$ and $[Cu(H_{-2}L^2)]\cdot 4H_2O$ by the route shown in Scheme 1.

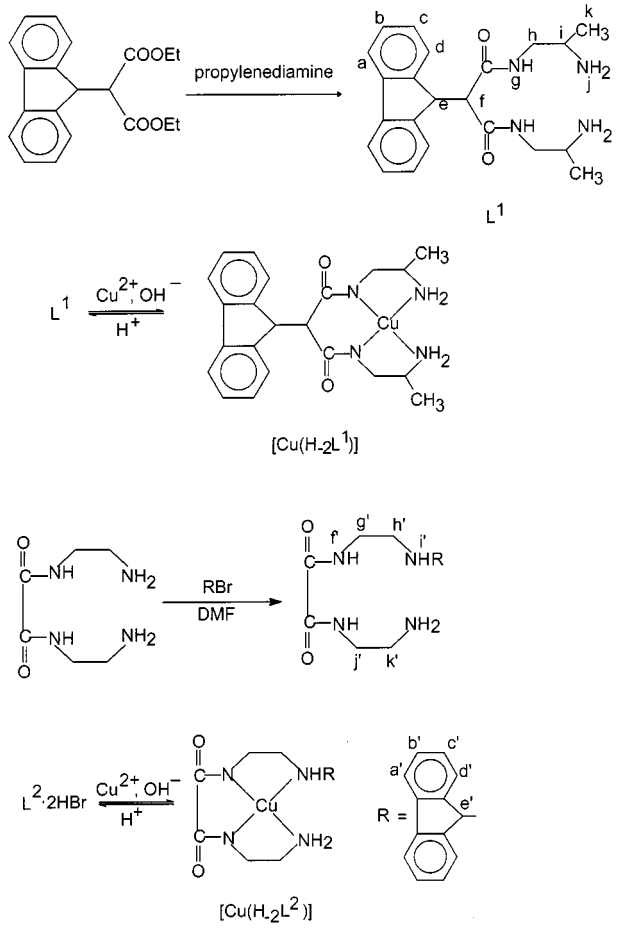

Scheme 1. Syntheses of ligands and complexes

[a] State Key Laboratory of Coordination Chemistry, Coordination Chemistry Institute, Nanjing University, Nanjing 210093, P. R. China
[b] Chemistry and Chemical Industry Department, Southeast University, Nanjing, 210009, P. R. China

  1434−1948/02/0303−0664 $ 17.50+.50/0 *Eur. J. Inorg. Chem.* **2002**, 664−670

It is interesting that L^1 and L^2 exhibit different fluorescent properties. The fluorescence of fluorenyl in L^1 is quenched by transfer of electrons from the metal center to the photoexcited state of fluorenyl during coordination of Cu^{II} or Ni^{II}. Conversely, fluorescence of L^2 is enhanced by coordination of transition metal ions. Their different fluorescent properties result from different positions of fluorenyl in the ligands. Because both ligands and complexes are water-soluble, they might have an application in biological analysis. To the best of our knowledge, the studies on enhancement of fluorescence of ligands by transition metal ions in aqueous solution are limited.[8]

Results and Discussion

Characterization

The values of molar conductivities of $[Cu(H_{-2}L^1)]\cdot 2H_2O$ and $[Cu(H_{-2}L^2)]\cdot 4H_2O$ in aqueous solution indicate that the amide protons are lost during coordination of the Cu^{2+} ion. In the IR spectra, both ligands exhibit two bands at about 760 and 740 cm^{-1} which are assigned to skeleton stretching vibration of the fluorene ring. The bands at 1660 cm^{-1} are assigned to the vibration of the carbonyl groups of L^1 or L^2 shifted by about 90 cm^{-1} during the coordination of Cu^{2+} ions. In the ^1H NMR spectrum of L^2 there are four groups of peaks at $\delta = 7.46-7.88$ assigned to the resonance absorption of protons of the fluorene ring, confirming linkage of the fluorenyl group to the dioxotetraamine unit. At $\delta = 2.96-3.62$ there are four groups of triple peaks assigned to the four methylene groups. The resonance absorption of protons on the nitrogen atoms disappeared due to exchange with heavy water. The ^1H NMR spectrum of the ligand L^1 is similar to that of L^2.

The ES-MS spectrum of L^2 that coexisted with the Cu^{2+} ion in methanol solution at pH = 9 is shown in Figure 1. The simplicity of the spectrum is attributed to the thermodynamic stability and kinetic inertness of the ligand. No obvious ligand fragmentation peaks were observed, showing that the ligand is quite stable under the ES-MS spectrum conditions.

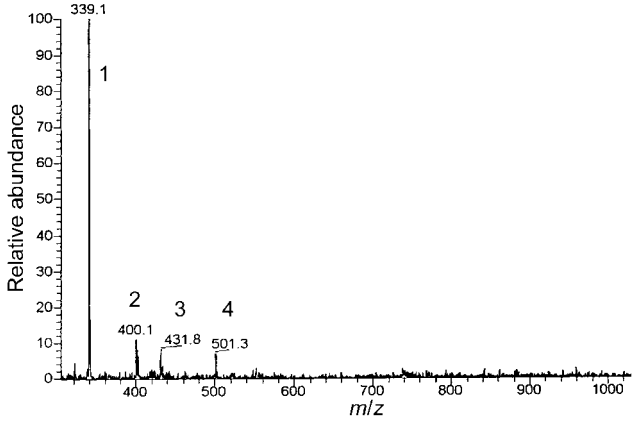

Figure 1. ES-MS spectrum of $L^2 + Cu^{2+}$ (1:1) system at pH = 9: 1. $[HL^2]^+$, 2. $[Cu(H_{-1}L^2)]^+$, 3. $[Cu(H_{-2}L^2)\cdot MeOH]^+$, 4. $[CuL^2(ClO_4)]^+$

Crystal Structure of $[Cu(H_{-2}L^1)]\cdot 2H_2O$

In Figure 2 the crystal structure of the copper(II) complex $[Cu(H_{-2}L^1)]\cdot 2H_2O$ is shown. Selected bond lengths and angles are listed in Table 1. From Figure 3 and Table 1 it can been seen that the copper(II) atom is situated in the center of a slightly distorted square composed of four nitrogen atoms. The distance between the plane and copper atom is 0.1628(4) Å. The distances of Cu−N are 1.941−2.022 Å. Two methyl groups are situated on the same side of the plane composed of four nitrogen atoms, and the carbon atoms (C-1, C-9) of the methyl groups deviate from the plane by 1.705(9) and 1.751(6) Å, respectively. The six-membered ring composed of N-2, Cu-1, N-3, C-6, C-5 and C-4 has a chair conformation. The fluorene ring is linked to the six-membered ring by the C-5 atom and forms a dihedral angle of 45.7 ° with the plane composed of N-2, N-3, C-6 and C-4. The complex was linked to the water molecules by the hydrogen bonds and formed a two-dimensional network structure.

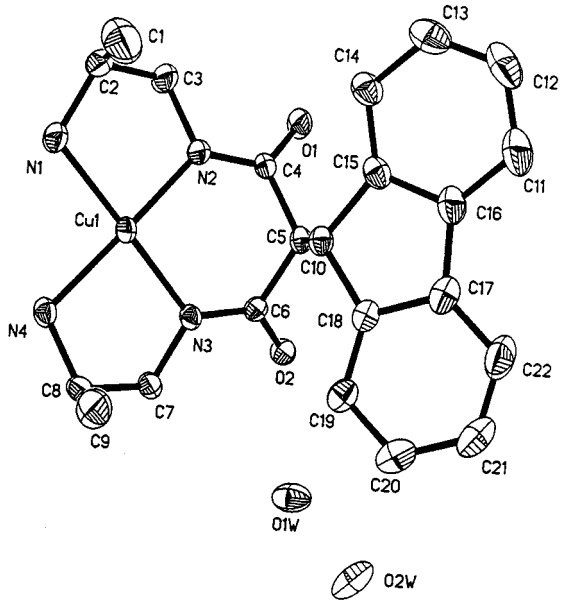

Figure 2. Crystal structure of $[Cu(H_{-2}L^1)]\cdot 2H_2O$

Table 1. Selected bond lengths [Å] and angles [°] of $[Cu(H_{-2}L^1)]$

Cu1−N1	2.012(4)	O1−C4	1.252(5)
Cu1−N2	1.941(3)	N1−C2	1.478(6)
Cu1−N3	1.955(3)	N2−C3	1.467(6)
Cu1−N4	2.022(3)	N2−C4	1.319(5)
N2−Cu1−N3	95.12(14)	C3−N2−Cu1	111.8(3)
N2−Cu1−N4	167.57(15)	C1−C2−N1	109.6(5)
N4−Cu1−N3	83.73(14)	N1−C2−C3	106.1(4)
N4−Cu1−N1	95.50(15)	C2−C3−N2	107.3(4)
N1−Cu1−N3	173.57(16)	C4−N2−C3	118.6(4)
C2−N1−Cu1	109.3(3)	O1−C4−N2	125.6(4)
C4−N2−Cu1	126.4(3)	O1−C4−C5	119.1(4)

Electrochemistry

The cyclic voltammetrical diagrams of $[Cu(H_{-2}L^1)]$ and $[Cu(H_{-2}L^2)]$ have similar features. During anodic scanning from 0−1.0 V, the ligands L^1 and L^2 do not show redox processes, but the two complexes display a pair of redox peaks. The separation between the anodic and cathodic peaks was 78−88 mV and the peak height ratio is near unit. A variation of the peak potential separation with scan rates (from 40 to 400 mVs^{-1}) was also observed. Furthermore, peak heights for the two complexes are proportional to the square roots of scan rates. The electron numbers of electrode oxidation reactions for $[Cu(H_{-2}L^1)]$ and $[Cu(H_{-2}L^2)]$ are 0.98 and 0.96 respectively, obtained by controlled potential analysis. These features are indicative of a one-electron quasi-reversible electrode process. Their values of $E_{1/2}$ are listed in Table 2.

Table 2. Half-wave potential $E_{1/2}$ (vs. SCE) for Cu^{III}/Cu^{II} redox process of $[Cu(H_{-2}L)]$ (L = L^1, L^2), pH = 9.8, scan rate 16 $mV{\cdot}s^{-1}$, Na_2SO_4 concentration = 0.5 $mol{\cdot}dm^{-3}$

	$[Cu(H_{-2}L^1)]$	$[Cu(H_{-2}L^2)]$
E_{pa} [V]	0.743	0.500
E_{Pc} [V]	0.655	0.422
ΔE [mV]	88	78
$E_{1/2}$ [V]	0.699	0.461

Stability of the Complexes

The pH-potentiometric titration curves of ligand L^1 and $L^2{\cdot}2HBr$ and that of the ligands plus metal ions(Cu^{2+}, Ni^{2+}, Co^{2+}, Zn^{2+}) are shown in Figure 3. In Figure 3 (a) all the curves 1−5 have two steps with defined inflection points. The first steps of all the curves are at $a = 2$ (a denotes the number of equivalents of base per mol of ligand), corresponding to free acid to be neutralized. The second step for the ligand L^1 (curve 1) is at $a \approx 4$, corresponding to protons of the amino cations to be neutralized. For the system of L^1 coexisting with the metal ions (curves 2−5), the second steps are at $a \approx 6$, corresponding to the formation of the predominant species $[M(H_{-2}L^1)]$.

The curves 6−8 in Figure 3 (b) are the titration curves of ligands L^2 and L^2 with the metal ions. At $a > 2$, the curves of the L^2 system are obviously different from those of the L^1 system. Curve 6 has two steps at $a = 3$ and $a = 4$, showing that the two amino nitrogen atoms have different abilities to bind protons. Two indistinct inflection points on curve 7 ($Cu^{2+} + L^2$) at $a = 4$ and $a = 5$ correspond to the formation of the dominant species $[CuL^2]^{2+}$ and $[Cu(H_{-1}L^2)]^{+}$, respectively. The obvious step of curve 8 at $a \approx 6$ shows that in the alkaline region $[Ni(H_{-2}L^2)]$ is the dominant species. Assuming that the above-mentioned species are formed, logarithms of the equilibrium constants, listed in Table 3, were obtained by curve fitting.

From Table 3 it can be seen that the stability sequence of the species [ML] and $[M(H_{-2}L)]$ (L = L^1 or L^2) is $Cu^{II} > Ni^{II} > Zn^{II} > Co^{II}$, being consistent with the Irving−Williams sequence. Stabilities of the complexes of L^2 in which an amino nitrogen atom is linked to a large fluorenyl group are lower than that of L^1. The species distribution curves of $L^1 + Cu^{2+}$ and $L^2 + Cu^{2+}$ systems are shown in Figure 4 and Figure 5, respectively.

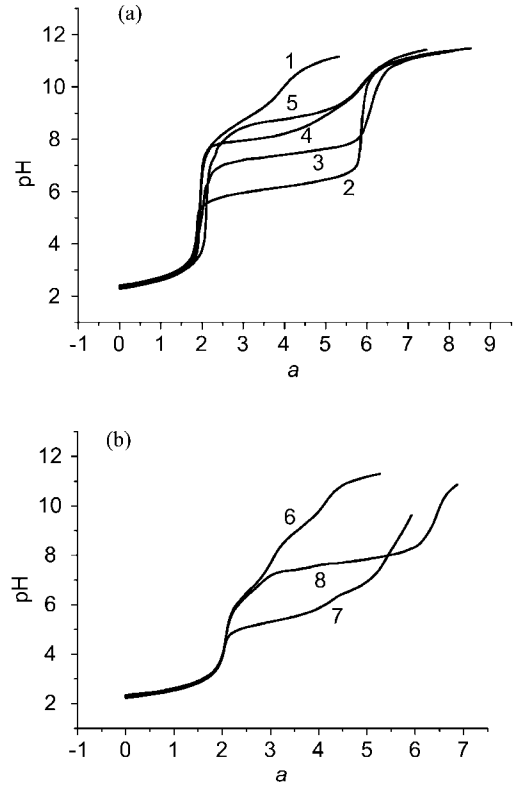

Figure 3. pH-potentiometric titration curves: (a) L^1 system, $L^1/M(NO_3)_2/HNO_3$ = 1:1:4; $L^1 = 1.8 \times 10^{-3}$ $mol{\cdot}dm^{-3}$: 1. M = none, 2. M = Cu^{2+}, 3. M = Ni^{2+}, 4. M = Zn^{2+}, 5. M = Co^{2+}; $L^2{\cdot}2HBr$ system, $L^2{\cdot}2HBr/HNO_3$ = 1:2; $L^2{\cdot}2HBr = 1.86 \times 10^{-3}$ $mol{\cdot}dm^{-3}$: 6. M = none, 7. $Cu^{2+} = 2.05 \times 10^{-3}$, 8. $Ni^{2+} = 2.08 \times 10^{-3}$ $mol{\cdot}dm^{-3}$

Fluorescent Properties of the Ligands in Aqueous Solution

The maximum fluorescence emission of L^1 in aqueous solution is located at 312 nm (pH = 9.0) by excitation of 280 nm. The intensity and position of the maximum emission remains constant at pH = 3−8. Figure 6 shows the dependence of the fluorescence intensity I_F (312 nm) and absorbance A (508 nm) of L^1 on the pH in the presence of Cu^{2+} ions. Both curves 1 and 2 show a typical sigmoidal shape. The dependence of the absorbance A on the pH is contrary to that of the fluorescence intensity. The curve of A vs. pH can be conveniently superimposed on the distribution diagram of $[Cu(H_{-2}L^1)]$ (Figure 4, curve 2), indicating that the formation of species $[Cu(H_{-2}L^1)]$ leads to quenching of the fluorescence by an electron transfer from the Cu^{II} center to the photoexcited state of the fluorenyl group Fl*. The fluorescent mechanism is similar to that of its analogs.[4,6] The electron-transfer process is described by Equation (1). The variation of potential of the electron transfer (ΔE_T) can be calculated by Equation (2).

Table 3. Logarithm of equilibrium constants of the ligands and complexes, 30±0.1 °C, KNO_3 concentration = 0.10 mol·dm^{-3}

Reaction[a]	H	Cu	Ni	Co	Zn[b]
$H^+ + L^1 \leftrightarrows (HL^1)^+$	9.11±0.01				
$2H^+ + L^1 \leftrightarrows (H_2L^1)^{2+}$	17.43±0.03				
$M^{2+} + L^1 \leftrightarrows [ML^1]^{2+}$		7.80±0.02	4.80±0.02		
$M^{2+} + L^1 \leftrightarrows [M(H_{-1}L^1)]^+ + H^+$		1.84±0.03		−5.85±0.02	−3.82±0.02
$M^{2+} + L^1 \leftrightarrows [M(H_{-2}L^1)] + 2\,H^+$		−4.12±0.03	−9.73±0.03	−14.39±0.03	−13.17±0.03
$H^+ + L^2 \leftrightarrows (HL^2)^+$	8.98±0.01				
$2H^+ + L^2 \leftrightarrows (H_2L^2)^{2+}$	15.51±0.03				
$M^{2+} + L^2 \leftrightarrows [ML^2]^{2+}$		7.68±0.02[b]	3.11±0.02[b]		
$M^{2+} + L^2 \leftrightarrows [M(H_{-1}L^2)]^+ + H^+$		1.68±0.03[b]			
$M^{2+} + L^2 \leftrightarrows [M(H_{-2}L^2)] + 2\,H^+$		−6.48±0.03[b]	−11.09±0.03[b]		

[a] For each system, two titrations were performed; during each titration more than 60 points were recorded. [b] At 25±0.1 °C.

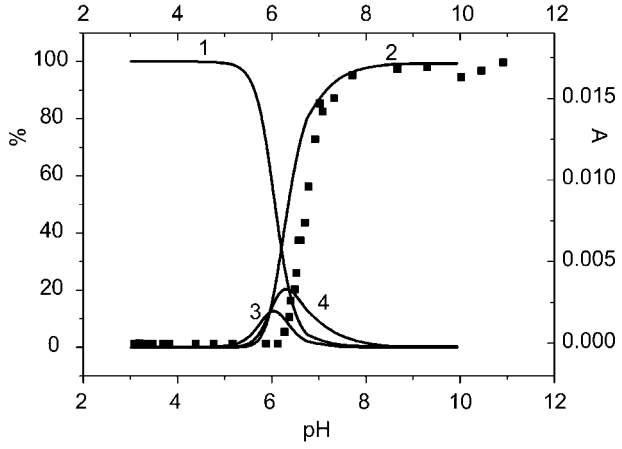

Figure 4. Species distribution curves and dependence of the absorbance A (■) on the pH for the $L^1 + Cu^{2+}$ system ($Cu^{2+} = L^1 = 2.6 \times 10^{-4}$ mol·dm^{-3}): 1. Cu^{2+}, 2. $[Cu(H_{-2}L^1)]$, 3. $[CuL^1]^{2+}$, 4. $[Cu(H_{-1}L^1)]^+$

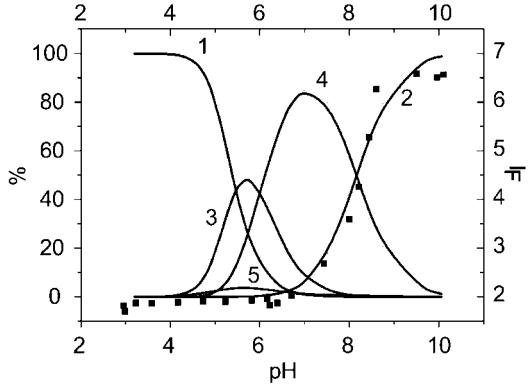

Figure 5. Species distribution curves and the dependence of the fluorescence intensity I_F (■) on the pH for the $L^2 + Cu^{2+}$ system ($Cu^{2+} = L^2 = 6.8 \times 10^{-5}$ mol·dm^{-3}): 1. Cu^{2+}, 2. $[Cu(H_{-2}L^2)]$, 3. $[CuL^2]^{2+}$, 4. $[Cu(H_{-1}L^2)]^+$, 5. $[HL^2]^+$

$$*Fl + [Cu^{II}(H_{-2}L^1)] \xrightarrow{\Delta E_T} Fl^- + [Cu^{III}(H_{-2}L^1)]^+ \quad (1)$$

$$\Delta E_T = E°(*Fl_{CT}) - E°(Cu^{III}/Cu^{II}) + E°(Fl/Fl^-) = 0.63\ V \quad (2)$$

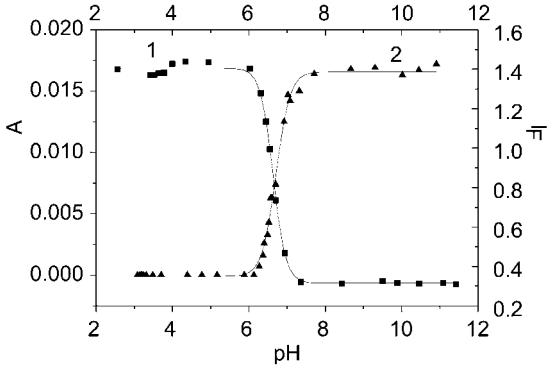

Figure 6. Dependence of fluorescence intensity I_F (1) and absorbance A (2) on the pH for an aqueous solution containing L^1 plus 1 equiv. Cu^{2+} ions

In Equation (2), the redox potential $E°(Fl/Fl^-)$ of the fluorenyl group linked to the dioxotetraaza moiety is −2.65 V, $E°(Cu^{III}/Cu^{II})$ is the redox potential obtained from cyclic voltammetrical experiments (0.699 V), and $E°(*Fl_{CT})$, the potential of the excited state, is 3.92 V, an approximation calculated from the energy of the emission band of the ligand.

The ΔE_T value of $[Cu(H_{-2}L^1)]$ is higher than that of $[Cu(H_{-2}L^3)]$[10b] (0.57 V) (L^3 denotes 6-(9*H*-fluoren-9-yl)-1,4,8,11-tetraazaundecane-5,7-dione), because in the former, two methyl groups that substituted two hydrogen atoms on the carbon atom of the ethylenediamine decreases the redox potential $E(Cu^{III}/Cu^{II})$ and increases the excited fluorescent potential of $[Cu(H_{-2}L^1)]$, thus favoring transfer of an electron from Cu^{II} to the fluorenyl group. The electron transfer behavior of L^1 in the presence of Ni^{2+} is similar to that in the presence of Cu^{2+}. For $[Ni(H_{-2}L^1)]$, ΔE_T (+0.57 V) was obtained by the same calculated method as that for $[Cu(H_{-2}L^1)]$. It is shown from Table 3 that the stability constants of the complexes of L^1 with Co^{II} and Zn^{II} are quite low, and the complexes $[M(H_{-2}L^1)]$ (M = Co, Zn) cannot be formed at pH ≤ 8.0, therefore the electron transfer cannot proceed. When the solution of ligand L^1 was adjusted to pH = 7.0 with NaOH and Ni^{2+} ions

were gradually added to it, no obvious decrease of I_F was observed (Figure 7). When Cu^{2+} ions were added to the same solution, I_F decreased linearly to a minimum value, corresponding to $n_{Cu}/n_L = 1$. Based on the above-mentioned results, L^1 could be employed as a fluorescent sensor to discriminate between Cu^{2+} and Ni^{2+}, as well as Cu^{2+} and Ni^{2+} ions from other divalent 3d metal ions.

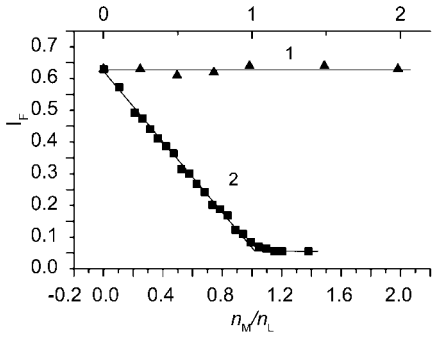

Figure 7. Plotting of I_F of H_2L^1 aqueous solution vs. n_M/n_L (M = Cu, Ni): 1. Ni^{2+} was added to a solution of H_2L^1 at pH = 7.0, 2. Cu^{2+} was added to the solution of 1.

Fluorescent properties of L^2 are different from L^1 and the fluorescent intensity of L^2 is low. A plot of I_F vs. pH in the presence of 1 equiv. of Cu^{2+} or Ni^{2+} ions is shown in Figure 8. In Figure 8, two systems display a similar fluorescent feature, when pH values of solutions are higher than 5.5. Fluorescence intensities increase with an increase of pH and reach a maximum value at pH $\approx$ 10. The curve of I_F vs. pH for systems of L^2 plus the Cu^{2+} ion can be superimposed on the distribution curve of $[Cu(H_{-2}L^2)]$ (Figure 5, curve 2), indicating that the formation of species $[Cu(H_{-2}L^2)]$ leads to an enhancement of the fluorescence. The distinction of the fluorescent properties between L^1 and of L^2 results from the difference of the structures. In L^2, a fluorenyl group substitutes a hydrogen atom of an amino group in the ligand and forms an imido group. The nitrogen atom of the imido group linked to the fluorenyl group can transfer its lone electron pair to a proximate excited fluorenyl group, quenching its fluorescence. When solutions of L^2 in the presence of metal ions were titrated with NaOH, an increase in the pH value led to binding of the metal ions. The electron transfer from the nitrogen atom to the fluorenyl group is suppressed, resulting in an enhancement of the fluorescence. The analogous mechanism has been reported by previous authors.[1,8,12] The detailed study on the fluorescence mechanism is in progress. Quantum yields of the ligand in the absence and presence of metal ions are listed in Table 4. From Table 4 it can be seen that L^2 has much lower quantum yields than L^1 in the absence of metal ions and the quantum yield of L^2 increases by about one order of magnitude upon binding of metal ions.

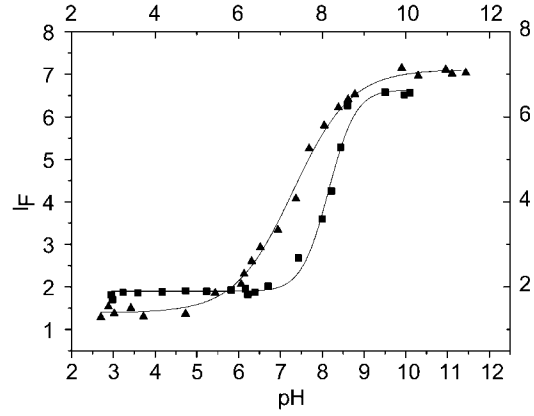

Figure 8. pH dependence of I_F for aqueous solutions containing L^2 plus metal ions; Cu^{2+} (■), Ni^{2+} (▲); $L^2 = Cu^{2+} = Ni^{2+} = 6.8 \times 10^{-5}$ mol·dm^{-3}

Table 4. Quantum yields of L^2 and L^2 plus metal ions (1:1) in aqueous solutions at 25 °C; $L^2 = Cu^{2+} = Ni^{2+} = 5 \times 10^{-5}$ mol·dm^{-3}

Sample	pH	Φ_u [a]
L^1	9.2	1.3×10^{-3}
L^2	9.2	2.0×10^{-4}
$Cu^{2+} + L^2$	5.0	5.2×10^{-4}
$Cu^{2+} + L^2$	9.2	2.7×10^{-3}
$Ni^{2+} + L^2$	5.0	2.6×10^{-4}
$Ni^{2+} + L^2$	9.2	3.4×10^{-3}
Trytophan[b]	7.2	0.14

[a] Deviation of measurement is ±15%. [b] Concentration of trytophan is 6.6×10^{-6} mol dm^{-3}.

It has been known for a long time that transition metal ions (especially Cu^{2+}) effectively quench the fluorescence of the systems by an electron transfer mechanism. Recently, Bharadwaj and co-workers[8] reported for the first time that Cu^{2+} and Ni^{2+} could enhance the fluorescence intensity of a ligand in THF/H_2O (9:1). In our systems, the enhancement of the fluorescence by Cu^{2+} and Ni^{2+} is carried out in aqueous solution. To the best of our knowledge, there are few reports[7] on enhancement of the fluorescence by transition metal ions in aqueous solution.

Experimental Section

Materials: Reagents and organic solvents were of reagent grade and purified prior to use. 9-Bromofluorene was prepared by literature methods.[13] Diethyl 2-(9*H*-fluoren-9-yl)malonate and *N*,*N*′-bis(2-aminoethyl)oxamide were synthesized by a method reported previously.[10b] Carbonate-free NaOH for pH titration was prepared by Powell's method.[14] $M(NO_3)_2 \cdot 6H_2O$ (M = Cu, Ni, Co, Zn) (reagent grade) were recrystallized from doubly distilled water and their stock solutions were standardized by titration with EDTA.

Spectral Measurements: IR spectra were measured as KBr discs with a Nicolet 5DX FT IR spectrophotometer. UV spectra were measured with an UV-3100 spectrophotometer. Luminescence spectra were recorded with an AB2 luminescence spectrometer.

Concentrations of metal ions and equivalent ligands in spectrophotometric titrations and in fluorimetric titrations were $2.6-4.3 \times 10^{-4}$ and $5.4-6.6 \times 10^{-5}$ mol·dm^{-3}, respectively. The solutions were deaerated for ca. 15 min before measurements. Quantum yields Φ of fluorescence were calculated by literature methods[15] using tryptophan as a standard. The quantum yield Φ_s of tryptophan is 0.14 in aqueous solution at 25 °C. Electrospray mass spectra (ES-MS) were obtained in positive mode with a Finnigan LCQ mass spectrograph. The diluted solutions were electrosprayed at a flow-rate of 2×10^{-4} dm^3·min^{-1} with a needle voltage of 4.5 kV. The mobile phase was a methanol solution. ^{1}H NMR spectroscopy was carried out with a Bruker AM500 spectrometer (TMS as internal reference).

Electrochemical Measurements: Cyclic voltammetry was carried out with a Model-270 electrochemical analysis system. A glassy carbon electrode was employed as working electrode, a saturated calomel electrode (SCE) as reference electrode and a platinum plate as auxiliary electrode. Experiments were performed under purified argon at 25 °C. Concentrations of the complexes were 1.0×10^{-3} to 1.0×10^{-4} mol·dm^{-3} in 0.2 mol·dm^{-3} potassium nitrate or in 0.5 mol·dm^{-3} sodium sulfate. The solutions were deaerated for ca. 15 min before applying the voltage. The half wave potentials $E_{1/2}$ were approximately calculated from $(E_{Pa} + E_{Pc})/2$. In a controlled potential coulometer, a platinum web electrode was employed as a working electrode instead of a glassy carbon.

pH Titration: The aqueous solutions containing L^1, $M(NO_3)_2$ and HNO_3 (1:1:4; M = Cu, Ni, Co, Zn) or L^2·2HBr, $M(NO_3)_2$ and HNO_3 (1:1:2; M = Cu, Ni) were titrated with carbonate-free 0.1598 mol·dm^{-3} NaOH using a microsyringe with a precision of ±2 μL in a sealed jacketed vessel at 30 °C under nitrogen. The pH values were measured with a Corning pH meter equipped with a glass/silver/silver chloride combination electrode with a precision of ±0.001 pH units. The combination electrode was standardized with buffer solutions of potassium hydrogen phthalate and sodium borate. The ionic strength was kept at 0.10 mol·dm^{-3} with KNO_3. The protonation constants of ligands were determined under the same conditions. The equilibrium constants were obtained by pH-potentiometric titrations. The protonation constants of the ligands were calculated by the PKAS program.[16] The equilibrium constants of complexes were calculated by using the program LEMIT,[17] which is based on the Newton−Raphson and Gauss−Newton method for minimizing U in Equation (3), where $C_{Hi}^{calcd.}$ and $C_{Hi}^{exp.}$ denote the calculated and experimental values of H^+ concentration at the ith point.

$$U = \sum_{i=1}^{n} (C_{Hi}^{\text{calcd.}} - C_{Hi}^{\text{exp.}})^2 \quad (3)$$

Preparation of Compounds

2,10-Diamino-6-(9*H*-fluoren-9-yl)-4,8-diazaundecane-5,7-dione (L^1): A mixture of diethyl 2-(9*H*-fluoren-9-yl)malonate (6.48 g, 0.02 mol) and freshly distilled propylenediamine (30 mL) was stirred at room temperature for two weeks. Excess propylenediamine was distilled off under reduced pressure. After cooling, the yellow residue was washed with ethanol and diethyl ether successively; L^1 (5.8 g, 76%) was obtained as a white solid. IR (KBr): ν_{max} = 3250 m (NH), 3030 w and 2930 w (CH), 1660 s (CO), 1540 s (NH), 760 m and 742 m cm^{-1} (C−C). UV (MeOH): λ_{max} (ε [dm^3·mol^{-1}·cm^{-1}]) = 266 (18700), 291 (4300) and 302 nm (4600). ^{1}H NMR (500 MHz, [D$_6$]DMSO, standard SiMe$_4$): δ = 0.92 (q, 6 H, *k*-CH$_3$), 2.91 (m, 2 H, *i*-CH), 2.98 (t, 4 H, *j*-NH$_2$), 3.06 (m, 7 H, *h*-CH$_2$, *f*-CH, *g*-CONH), 4.35 (d, 1 H, *e*-CH-Ar), 7.24 (m, 2 H, *c*-Ar-H), 7.39 (t, 2 H, *b*-Ar-H), 7.43 (d, 2 H, *d*-Ar-H), 7.86 (d, 2 H, *a*-Ar-H). $C_{22}H_{28}N_4O_2$ (380.5): calcd. C 69.45, H 7.42, N 14.72; found C 69.23, H 7.28, N 14.54.

1-(9*H*-Fluoren-9-yl)-1,4,7,10-tetraazadecane-5,6-dione Hydrogen Bromide (L^2·2HBr): To a solution of *N*,*N*′-bis(2-aminoethyl)oxamide (1.4 g, 0.008 mol) in DMF (30 mL), a solution of 9-bromofluorene (1.97 g, 0.008 mol) in DMF(20 mL) was added dropwise whilst stirring at 80 °C. After heating for 5 h at 80 °C, the mixture was cooled and filtered. The filtrate was added dropwise ice-cold water (400 mL). After filtering, the filtrate was concentrated to almost dryness and 30 mL of diethyl ether was added. The resultant product was separated and washed with diethyl ether, and 0.5 g of white solid was obtained. The white solid was recrystallized from 95% ethanol, and L^2·2HBr (0.4 g, 10.0%) was obtained. IR (KBr): ν_{max} = 3500 m to 2500 b (NH_3^+), 1660 s (CO), 1580 s (NH), 1520 s, 1440 s, 1070 m, 765 m and 745 m cm^{-1} (C−C). UV (MeOH): λ_{max} (ε [dm^3·mol^{-1}·cm^{-1}]) = 268 (15000), 294 (4130) and 304 (3730). ^{1}H NMR(500 MHz, D$_2$O, standard SiMe$_4$): δ = 2.96 (2 H, t, *j*′-CH$_2$NCO), 3.21 (2 H, t, *g*′-CH$_2$NCO), 3.51 (2 H, t, *h*′-CH$_2$-NAr), 3.62 (2 H, t, *k*′-CH$_2$N$^+$), 5.56 (1 H, s, *e*′-CH), 7.46 (2 H, t, *c*′-Ar-H), 7.59 (2 H, t, *b*′-Ar-H), 7.74 (2 H, d, *d*′-Ar-H), 7.88 (2 H, d, *a*′-Ar-H). $C_{19}H_{24}Br_2N_4O_2$ (500.2): calcd. C 45.62, H 4.84, N 11.20; found C 45.96, H 5.11, N 11.45.

[Cu(H$_{-2}$L^1)]·2H$_2$O: To a solution of L^1 (1.14 g, 3.0 mmol) in water (50 mL), $CuSO_4$·5H$_2$O (0.75 g, 3.0 mmol) was added. Whilst stirring, the mixture was adjusted to pH = 10 with dilute $Ba(OH)_2$ solution. After heating at 80 °C for 2 h, the mixture was filtered. The filtrate was concentrated and cooled; purple-red crystals of [Cu(H$_{-2}$L^1)]·2H$_2$O (0.32 g, 22.3%) were obtained. IR: ν_{max} = 3350 m (OH), 3200 m (NH), 3100 m, 2950 w and 2900 w (CH), 1570 vs (C=O), 760 w and 730 w cm^{-1}(C−C). UV (H$_2$O): λ_{max} (ε [dm^3·mol^{-1}·cm^{-1}]) = 265 (4280), 274 (3440), 291 (1210), 302 (1120) and 504 (69) nm. Λ_m (H$_2$O, 25 °C) = 68.75 S·cm^2·mol^{-1}. $C_{22}H_{30}CuN_4O_4$ (478.1): calcd. C 55.27, H 6.33, N 11.72, Cu 13.27; found C 55.61, H 6.25, N 11.57, Cu 13.13.

[Cu(H$_{-2}$L^2)]·4H$_2$O: L^2·2HBr (0.25 g, 0.5 mmol) and $CuSO_4$·5H$_2$O (0.125 g, 0.5 mmol) were dissolved in water (20 mL). The solution was adjusted to pH = 10 with a dilute solution of $Ba(OH)_2$ whilst stirring. After stirring for 1 h at 80 °C, the solution was cooled and filtered. The filtrate was concentrated and a purple solid of [Cu(H$_{-2}$L^2)]·4H$_2$O (0.12 g, 50.9%) was obtained. IR (KBr): ν_{max} = 3350 m (OH), 3200 m (NH), 2900 w (CH), 1651 s (CO), 1600 s (CO), 1100 m, 745 m and 620 cm^{-1} (C−C). UV (H$_2$O): λ_{max} (ε [dm^3·mol^{-1}·cm^{-1}]) = 268 (15000), 294 (4130), 304 (3730) and 536 (154). Λ_m (H$_2$O, 25 °C) = 69.10 S·cm^2·mol^{-1}. $C_{19}H_{28}CuN_4O_6$ (472.0): calcd. C 48.36, H 5.98, N 11.87; found C 48.54, H 6.08, N 11.57.

X-ray Structure Determination of [Cu(H$_{-2}$L^1)]·2H$_2$O: Crystal data: $C_{22}H_{30}CuN_4O_4$, M = 478.04, monoclinic, space group $P2_1/n$, a = 17.264(4) Å, b = 7.6627(16) Å, c =19.559(4) Å, β = 114.582(15) °, V = 2352.9(8) Å^3, $D_{calcd.}$ = 1.349 Mg·m^{-3}, F(000) = 1004, Z = 4, graphite-monochromated Mo-K radiation (λ = 0.71073 Å), μ = 0.962 mm^{-1}, T = 293(2) K. Data collection and processing: A crystal of [Cu(H$_{-2}$L)]·2H$_2$O with dimensions 0.40 × 0.30 × 0.30 mm, wrapped with resin, was mounted on a glass fiber and used for structure determination. The intensities were collected at 293 K with a Siemens *P*4 four-circle diffractometer with θ/2θ scan mode with a variable scan speed of 4.0−60.0 min^{-1} in ω. A total of 5316 reflections (4129 unique) were collected in the range of

$2.06° < \theta < 25.0°$. The data were corrected for Lorentz and polarization effects during data reduction using XSCANS.[18] Structure analysis and refinement: The structure was solved by direct methods. All non-hydrogen atoms were refinedanisotropically on F^2 by full-matrix least-squares methods. The hydrogen atoms were placed in calculated positions assigned fixed isotropic thermal parameters at 1.2 times the equivalent isotropic U of the atoms to which they are attached and allowed to ride on their respective parent atoms. The contributions of these hydrogen atoms were included in the structure-factor calculations. The final least-squares cycle gave $R = 0.0542$, $Rw = 0.1280$ and $GOF = 1.075$. The maximum and minimum peaks corresponded to $+0.665$ and -0.290 eÅ^{-3}, respectively. All computations were carried out using the SHELXTL PC program package.[19] Crystallographic data for the the crystal structure of $[Cu(H_{-2}L^1)]\cdot 2H_2O$ have been deposited with the Cambridge Crystallographic Data Centre as supplementary publication no. CCDC-163292. Copies of the data can be obtained free of charge on applicaton to CCDC, 12 Union Road, Cambridge CB2 1EZ, UK [Fax: (internat.) + 44-1223/336-033; E-mail: deposit@ccdc.cam.ac.uk].

Acknowledgments

The project was supported by the Natural Science Foundation of China and 211 Project of China.

[1] A. P. de Silva, H. Q. N. Gunaratne, T. Gunnlaugsson, A. J. M. Huxley, C. P. McCoy, J. T. Rademacher, T. E. Rice, *Chem. Rev.* **1997**, *97*, 1515.
[2] G. D. Santis, L. Fabbrizzi, M. Licchelli, A. Poggi, A. Taglietti, *Angew. Chem. Int. Ed. Engl.* **1996**, *35*, 202.
[3] [3a] E. Kimura, *Pure Appl. Chem.* **1986**, *58*, 1461. [3b] E. Kimura, *Pure Appl. Chem.* **1989**, *61*, 823. [3c] E. Kimura, T. Koike, *Chem. Soc. Rev.* **1998**, *27*, 179. [3d] G. E. Jackson, P. W. Linder, A. Voye, *J. Chem. Soc., Dalton Trans.* **1996**, 4605. [3e] Q. H. Luo, S. R. Zhu, M. C. Shen, S. Y. Yu, Z. Zhang, X. Y. Huang, Q. J. Wu, *J. Chem. Soc., Dalton Trans.* **1994**, 1873.
[4] L. Fabbrizzi, A. Poggi, *Chem. Soc. Rev.* **1995**, 197.
[5] L. Fabbrizzi, M. Licchelli, P. Pallavicini, D. Sacchi, A. Taglietti, *Analyst* **1996**, *121*, 1763.
[6] L. Fabbrizzi, M. Licchelli, P. Pallavicini, A. Perotti, D. Sacchi, *Angew. Chem. Int. Ed. Engl.* **1994**, *33*, 1975.
[7] F. Bolletta, I. Costa, L. Fabbrizzi, M. Licchelli, M. Montalti, P. Pallavicini, L. Prodi, N. Zaccheroni, *J. Chem. Soc., Dalton Trans.* **1999**, 1381.
[8] P. Ghosh, P.K. Bharadwaj, J. Roy, S. Ghosh, *J. Am. Chem. Soc.* **1997**, *119*, 11903.
[9] P. V. Bernhardt, B. M. Flanagan, M. J. Riley, *J. Chem. Soc., Dalton Trans.* **1999**, 3579.
[10] [10a] L. Fabbrizzi, I. Faravelli, G. Francese, M. Licchelli, A. Perotti, A. Taglietti, *Chem. Commun.* **1998**, 971. [10b] L. J. Jiang, Q. H. Luo, C. Y. Duan, M. C. Shen, H. W. Hu, Y. J. Liu, *Inorg. Chim. Acta* **1999**, *295*, 48.
[11] M. Kodama, E. Kimura, *J. Chem. Soc., Dalton Trans.* **1981**, 694.
[12] V. Amendola, L. Fabbrizzi, P. Pallavicini, L. Parodi, A. Perotti, *J. Chem. Soc., Dalton Trans.* **1998**, 2053.
[13] J. R. Sampey, E. E. Reid, *J. Am. Chem. Soc.* **1947**, *69*, 234.
[14] J. E. Powell, M. A. Hiller, *J. Chem. Educ.* **1957**, *34*, 330.
[15] D. F. Eaton, *Pure Appl. Chem.* **1988**, *60*, 1107.
[16] A. E. Martell, R. J. Motekaitis, *Determination and Use of Stability Constants*, 2nd ed., VCH Publishers, New York, **1992**, p. 129.
[17] Q. H. Luo, M. C. Shen, Y. Ding, X. L. Bao, A. B. Dai, *Talanta* **1990**, *37*, 357.
[18] Siemens, *XSCANS (Version 2.1)*, Siemens Analytical X-ray Instruments Inc. Madison USA, **1994**.
[19] Siemens, *SHELXTL (Version 5.0) Reference Manual*, Siemens Industrial Automation Inc. analytical Instrumentation, USA, **1995**.

Received August 21, 2001
[I01320]